

Supporting Information

Sato et al. 10.1073/pnas.1109088108

SI Methods

Preparation of the HOIL-1L NZF Domain. The gene encoding the Npl4 zinc finger (NZF) domain of mouse HOIL-1L (residues 192–250) was PCR amplified from a mouse cDNA library. The amplified gene was cloned into the pCold-GST expression vector (1) with *NdeI* and *XhoI* sites to produce N-terminal GST fusion protein and confirmed by DNA sequencing. *Escherichia coli* strain Rosetta™ (DE3) cells (Invitrogen) were transformed with the expression vector and cultured in LB media containing 100 mg/L ampicillin at 37 °C. When the optical density at 600 nm of the culture reached approximately 0.5, the culture was incubated for 30 min at 15 °C. Thereafter, isopropyl- β -D-thiogalactopyranoside (IPTG) was added to a final concentration of 0.3 mM to induce protein expression for 24 h at 15 °C. The cells were collected by centrifugation at $8,000 \times g$ for 15 min and disrupted by sonication in phosphate buffered saline (PBS), containing 1 mM dithiothreitol (DTT), 1 mM phenylmethylsulfonyl fluoride (PMSF), and 0.5% Triton X-100. The lysates were centrifuged at $30,000 \times g$ for 60 min, and the supernatants were then loaded onto a Glutathione Sepharose FF column (GE Healthcare) that had been preequilibrated with PBS containing 1 mM DTT and 0.5% Triton X-100. The column was washed with PBS containing 1 mM DTT and 0.5% Triton X-100 and then with PBS containing 1 mM DTT. GST fusion proteins were eluted with 50 mM Tris-HCl buffer (pH 8.0) containing 200 mM NaCl, 1 mM DTT and 15 mM reduced glutathione. The GST tags were cleaved by Turbo3C (HRV3C) protease (Accelagen), and the samples were dialyzed against 50 mM Tris-HCl buffer (pH 8.0), containing 40 mM NaCl and 1 mM DTT. The proteins were loaded onto a ResourceQ anion exchange column (GE Healthcare) preequilibrated with 50 mM Tris-HCl buffer (pH 8.0) containing 40 mM NaCl and 1 mM DTT, and were eluted with a linear gradient of 0–1 M NaCl. The cleaved GST tags were then removed by chromatography on a Glutathione Sepharose FF column (GE Healthcare). The samples were loaded onto a Superdex 75 16/60 (prep grade) column (GE Healthcare) preequilibrate with 10 mM Tris-HCl buffer (pH 7.2) containing 50 mM NaCl and 5 mM β -mercaptoethanol. The fractions rich in the purified proteins were collected for crystallization.

Preparation of Linear Ub₂. The genes encoding mouse linear Ub₂ was cloned into pT7-7 (United States Biochemical Corp) expression vector. *E. coli* strain Rosetta (DE3) cells (Invitrogen) were transformed with the expression vector to produce linear Ub₂. The transformed *E. coli* cells were cultured in LB media containing 100 mg/L ampicillin at 37 °C. When the optical density at 600 nm of the culture reached approximately 0.5, IPTG was added to a final concentration of 0.3 mM to induce protein expression. After expression for 17 h at 20 °C, cells were collected by centrifugation at $8,000 \times g$ for 15 min and disrupted by sonication in 50 mM ammonium acetate (pH 4.5) buffer containing 2 mM DTT, 1 mM EDTA, and 1 mM PMSF. The cleared lysate was incubated at 70 °C for 5 min to denature proteins from *E. coli*, which were precipitated by centrifugation at $30,000 \times g$ for 20 min. The supernatant was loaded onto SP Sepharose FF (GE Healthcare) preequilibrated with 50 mM ammonium acetate (pH 4.5) buffer containing 2 mM DTT and 0.1 mM EDTA. Linear Ub₂ was eluted with a linear gradient of 0–500 mM NaCl, and further fractionated by HiLoad Superdex75 (GE Healthcare) size-exclusion column with 50 mM Tris-HCl (pH 7.6) buffer containing 2 mM DTT and 0.1 mM EDTA. Purified linear Ub₂ was

concentrated to 24 g/L and stored at –80 °C until use. K48- and K63-Ub₂ were prepared as described previously (2).

Crystallization. To prepare the HOIL-1L NZF•linear Ub₂ complex, a 2-fold molar excess of HOIL-1L NZF was incubated at 4 °C overnight with linear Ub₂. The HOIL-1L NZF•linear Ub₂ complex was loaded onto a HiLoad Superdex75 size-exclusion column (GE Healthcare) preequilibrated with 10 mM Tris-HCl buffer (pH 7.2), 50 mM NaCl and 5 mM β -mercaptoethanol, to remove unbound linear Ub₂. Purified HOIL-1L NZF•linear Ub₂ complex was concentrated to 10.5 g/L, by using an Amicon Ultra-15 3,000 MWCO filter (Millipore), following the manufacturer's instructions. Initial crystallization screening was performed using the sitting drop vapor diffusion method at 20 °C, with a Mosquito® liquid-handling robot (TTP Lab Tech). We tested about 500 conditions, using crystallization reagent kits supplied by Hampton Research, and initial hits were further optimized. The crystals of the 1.6-Å resolution complex were obtained from mother liquid containing 1.3 M tri-sodium citrate, 90 mM-HEPES-NaOH buffer (pH 7.5), and 100 mM potassium sodium tartrate. The crystals of the 1.9-Å resolution complex were obtained from mother liquid containing 1.45 M triammonium citrate (pH 7.0) and 3% 1,6-diaminohexane. The crystal of the 1.7-Å resolution complex belonged to space group $P4_32_12$, with unit cell dimensions of $a = b = 104.9$ Å, $c = 170.4$ Å. The crystal of the 1.9-Å resolution complex belonged to space group $P6$, with unit cell dimensions of $a = b = 113.7$ Å, $c = 75.7$ Å.

Structure Determination. Diffraction datasets were collected at beamline BL41XU in SPring-8 (Hyogo, Japan) and processed with HKL2000 (3) and the CCP4 program suite (4). The complex structures were determined by molecular replacement using the program MolRep (5). The crystal structures of the TAB2 NZF domain and the distal ubiquitin moiety in the TAB2•K63-Ub₂ complex [Protein Data Bank (PDB) ID code 3A9J] and monoUb (PDB ID code 1UBQ) were used as search models for the HOIL-1L NZF•linear Ub₂ complex structure of the $P6$ crystal. The HOIL-1L NZF•linear Ub₂ complex structure of the $P6$ crystal was used as a search model for the HOIL-1L NZF•linear Ub₂ complex structure of the $P4_32_12$ crystal. Two and four HOIL-1L NZF•linear Ub₂ complexes were found in the asymmetric unit of the $P6$ and $P4_32_12$ crystals, respectively. Atomic models were corrected by using COOT (6) with careful inspection. Refinement was carried out by using PHENIX (7), including temperature factor, positional, and translation, libration, and screw-rotation (TLS) refinement, treating each protein molecule as one TLS group. The final models have excellent stereochemistry with R_{free} values of 0.227 and 0.211 at 1.9- and 1.7-Å resolutions for the $P6$ and $P4_32_12$ complexes, respectively. Data collection, phasing and refinement statistics are shown in Table S1. All molecular graphics were prepared with PyMOL (DeLano Scientific; <http://www.pymol.org>).

Surface-Plasmon Resonance (SPR) Analysis. GST-fused monoubiquitin and linear Ub₂ for SPR analyses were purified by Glutathione Sepharose FF and ResourceQ anion exchange columns (GE Healthcare). GST-fused K48-Ub₂ was synthesized from D77 ubiquitin and GST-fused K48R ubiquitin. GST-fused K63-Ub₂ was synthesized from D77 ubiquitin and GST-fused K63R ubiquitin. Ubiquitin conjugation reactions were performed as described previously (8). NZFs of mouse HOIL-1L, TAB2, Npl4 and SHANK-associated RH domain interacting protein (SHARPIN)

and Ub-binding of ABINs and NEMO (UBAN) of mouse NF- κ B essential modulator (NEMO) were overproduced as GST-fusion proteins in *E. coli* strain Rosetta™ (DE3) (Invitrogen) and purified by Glutathione Sepharose FF and ResourceQ anion exchange columns (GE Healthcare). After cleavage of the GST tag, the proteins were further purified by HiLoad Superdex200 size-exclusion column (GE Healthcare) and passed through Glutathione Sepharose FF to completely remove the residual GST proteins. Experiments were carried out on a Biacore T200 instrument (GE Healthcare), equilibrated at 25 °C in HBS-P buffer including 10 mM-HEPES (pH 7.4), 150 mM NaCl and 0.05% surfactant P 20, using a Sensor Chip CM5 (GE Healthcare). GST antibody (GE Healthcare) was covalently immobilized on the sensor chip at a density of about 14,000 resonance units (RU), and GST-fused monoUb and diUb were captured on the sensor chip at a density of 1,300–1,500 RU. Ub receptors were then injected for 60 s at a flow rate of 10 mL/min. Dissociation constants (K_d) were computed by fitting to a 1:1 interaction model using Biacore T200 evaluation software (GE Healthcare). The assay was carried out three times for each mutant. Data are presented as means \pm SD. Details of the constructs used in SPR analyses are shown in Table S2.

GST Pull-Down Assay. GST-fused NZFs of mouse HOIL-1L, TAB2, Npl4, and SHARPIN for pull-down analyses were overproduced in *E. coli* strain Rosetta™ (DE3) (Invitrogen), and purified by Glutathione Sepharose FF and Resource Q anion exchange columns (GE Healthcare). Mutations were generated by PCR. One hundred micrograms of the GST-fused wild type and mutants of NZFs were immobilized on Glutathione Sepharose FF beads (GE healthcare), and then incubated with 50 μ g of linear, K48-, or K63-Ub₂ for 15 min at 4 °C in 25 mM Tris-HCl buffer (pH 7.2) containing 20 μ M zinc chloride, 1 mM DTT, 100 mM NaCl, and 0.1% Triton X-100. The beads were washed with the same buffer thrice. The Ub₂ molecules bound to the beads were released by boiling in SDS loading buffer and analyzed by SDS-PAGE. The gels were stained with Coomassie Brilliant Blue.

Luciferase Assay. HEK293T cells were transfected with pGL4.32 [Luc2P/NF- κ B-RE/Hygro] (Promega), pGL4.74 [hRLuc/TK] (Promega), pcDNA3.1 Myc-human HOIP, and pcDNA3.1 con-

taining the wild type or mutants of human HOIL-1L-His-HA (Table S2). At 24 h after transfection with the appropriate plasmids, cells were lysed and luciferase activity was measured in a Lumat luminometer (Berthold) using the Dual-Luciferase reporter assay system (Promega).

In Vitro Ubiquitination of NEMO by the Linear Ubiquitin Chain Assembly Complex (LUBAC). Recombinant baculoviruses encoding human HOIL-1L, HOIL-1L(Δ NZF), HOIL-1L(T203/R210A), and His₆-HOIP were generated using the Bac-PAC6 baculovirus expression system (BD Biosciences). The HOIP•HOIL-1L complex was prepared from HiFive cells infected with the appropriate combination of the recombinant baculoviruses, followed by purification using an Ni-NTA (Qiagen) column. Human MBP-NEMO was overproduced in *E. coli* using pMAL-c2x vector (New England Biolabs) and purified by amylose resin (New England Labs). Reaction mixtures contained 5 μ g/mL of E1, 2.5 μ g/mL of Ubc5c, 5 μ g/mL of the HOIP/HOIL-1L complex or its mutants, 12.5 μ g/mL of MBP-NEMO, and 250 μ g/mL of ubiquitin were incubated at 37 °C for 1 h in 20 mM Tris-HCl (pH 7.5), 10 mM MgCl₂, 1 mM DTT, and 2 mM ATP. Samples were subjected to SDS-PAGE and Western blotting with anti-MBP-antibody (Santa Cruz).

In Vivo Ubiquitination of NEMO by LUBAC. HEK293T cells were transfected with pcDNA3.1-FLAG-NEMO, pcDNA3.1-Myc-human HOIP, and pcDNA3.1-human HOIL-1L-HA (Invitrogen). At 2 d after transfection with the appropriate plasmids, cells were lysed in 50 mM Tris-HCl (pH 7.5) buffer, containing 150 mM NaCl, 1% Triton X-100, and 2 mM PMSF. The lysate was incubated with antiFLAG antibody (Sigma) for 90 min on ice, and then immobilized on the proteinA Sepharose beads (GE Healthcare). The beads were washed with the same buffer four times. Samples were separated by SDS-PAGE and transferred to PVDF membranes. After blocking in TBS containing 0.1% Tween-20 and 5% skimmed milk, the membrane was incubated with the appropriate primary antibodies, followed by incubation with secondary antibodies. The membrane was visualized using enhanced chemiluminescence and analyzed by LAS4000 mini (GE Healthcare).

- Hayashi K, Kojima C (2008) pCold-GST vector: A novel cold-shock vector containing GST tag for soluble protein production. *Protein Expr Purif* 62:120–127.
- Sato Y, et al. (2008) Structural basis for specific cleavage of Lys 63-linked polyubiquitin chains. *Nature* 455:358–362.
- Otwinowski Z, Minor W (1997) Processing of X-ray diffraction data collected in oscillation mode. *Methods Enzymol* 276:307–326.
- Collaborative Computational Project N (1994) The CCP4 suite: Programs for protein crystallography. *Acta Crystallogr D Biol Crystallogr* 50:760–763.
- Vagin A, Teplyakov A (1997) MOLREP: An automated program for molecular replacement. *J Appl Cryst* 30:1022–1025.
- Emsley P, Cowtan K (2004) Coot: Model-building tools for molecular graphics. *Acta Crystallogr D Biol Crystallogr* 60:2126–2132.
- Zwart PH, et al. (2008) Automated structure solution with the PHENIX suite. *Methods Mol Biol* 426:419–435.
- Kulathu Y, Akutsu M, Bremm A, Hofmann K, Komander D (2009) Two-sided ubiquitin binding explains specificity of the TAB2 NZF domain. *Nat Struct Mol Biol* 16:1328–1330.
- Sato Y, Yoshikawa A, Yamashita M, Yamagata A, Fukai S (2009) Structural basis for specific recognition of Lys 63-linked polyubiquitin chains by NZF domains of TAB2 and TAB3. *EMBO J* 28:3903–3909.

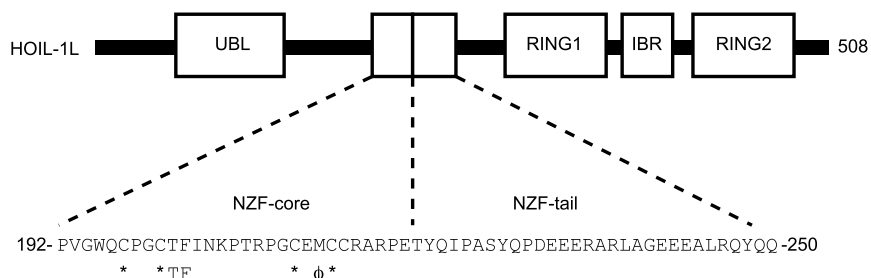


Fig. S1. Domain diagram of the HOIL-1L subunit. Abbreviations are as follows: UBL, ubiquitin like; RING, really interesting new gene; IBR, in between RING. The conserved cysteine residues are shown by asterisks. The TF/ Φ motif is shown below the sequence.

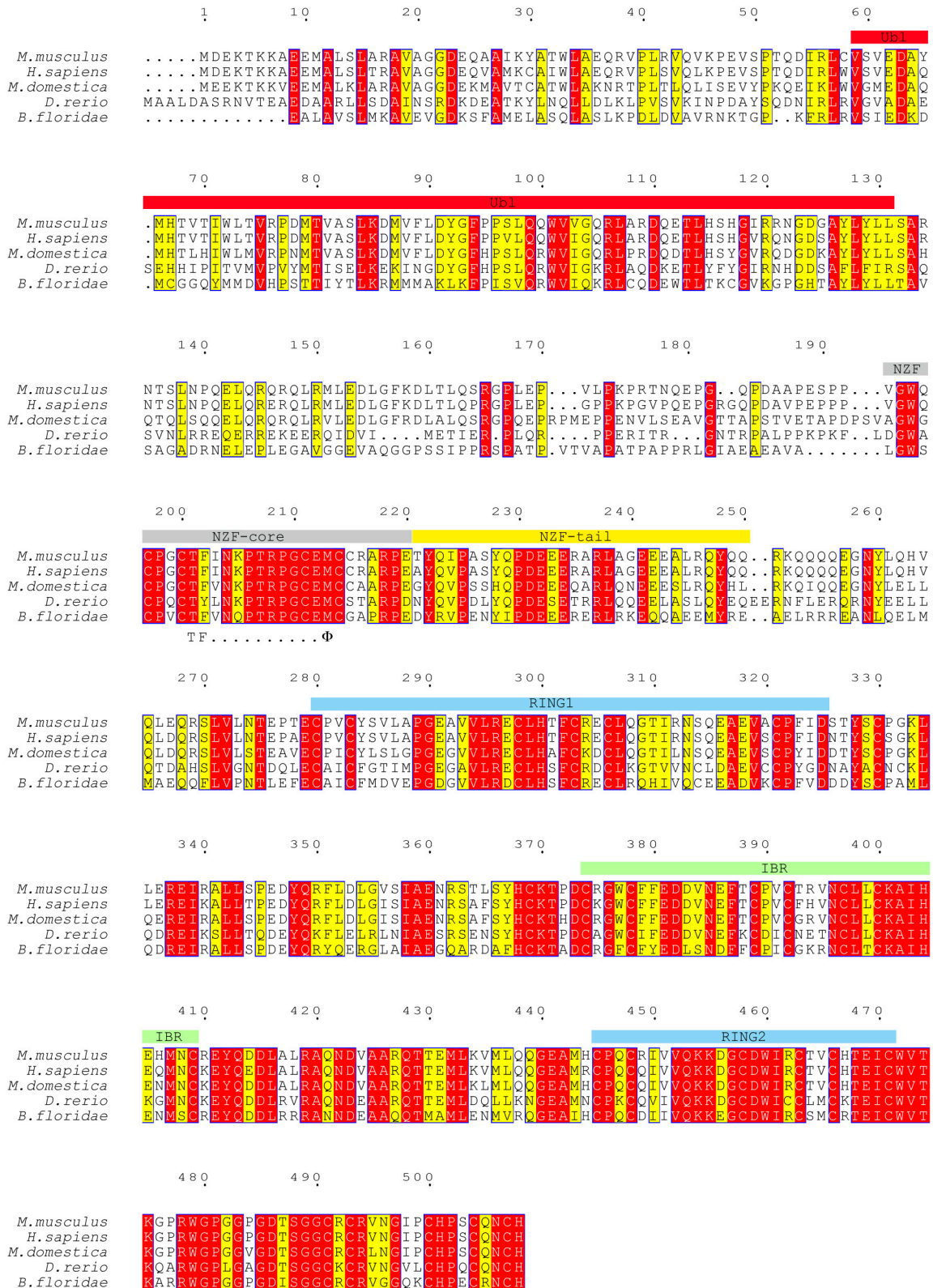


Fig. S2. Comparison of the amino acid sequences of HOIL-1L from representative organisms; 100% and more than 70% identical residues are highlighted by red and yellow background, respectively. The domain diagram of mouse HOIL-1L is shown above the alignment. The TF/Φ motif is shown below the alignment.

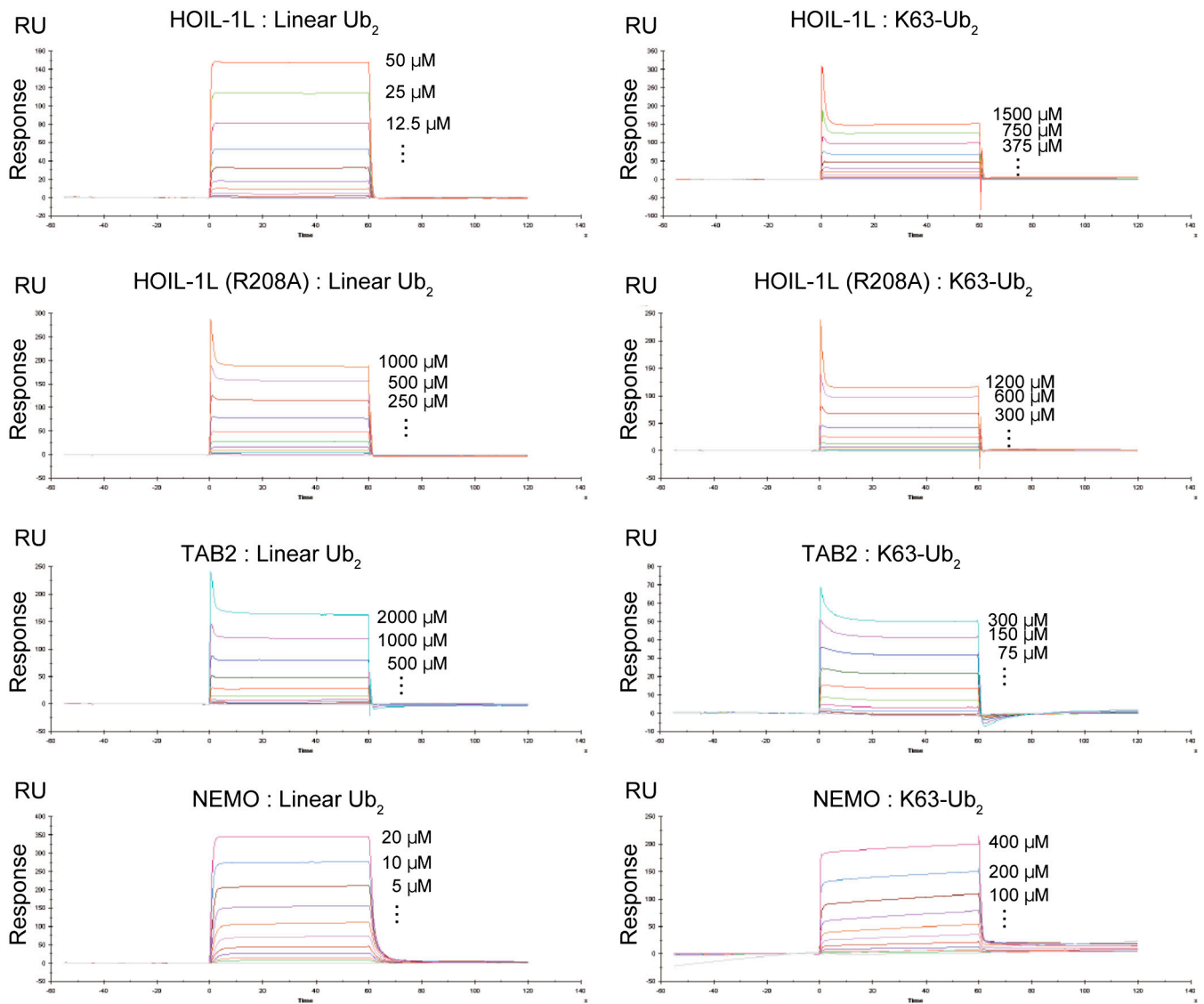


Fig. 53. Sensorgrams of SPR experiments. GST-fused diubiquitin was immobilized on the sensor chip as ligands, and then ubiquitin-binding proteins were injected as analytes. Measurements were done thrice at 10 different concentrations for each analyte.

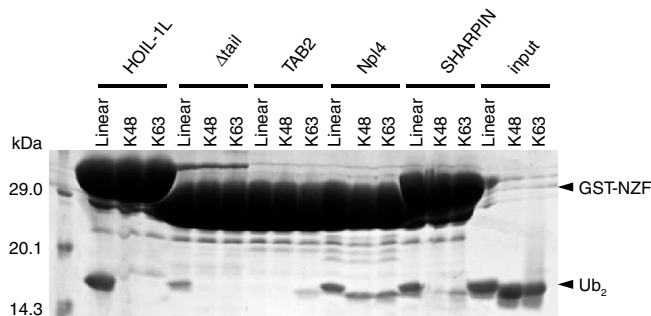


Fig. 54. Pull-down assays to assess ubiquitin-chain binding. Pull-down assays using GST-fused HOIL-1L, TAB2, Npl4, and Sharpin NZF domains to assess their ability to bind linear, K48-, and K63-Ub₂.

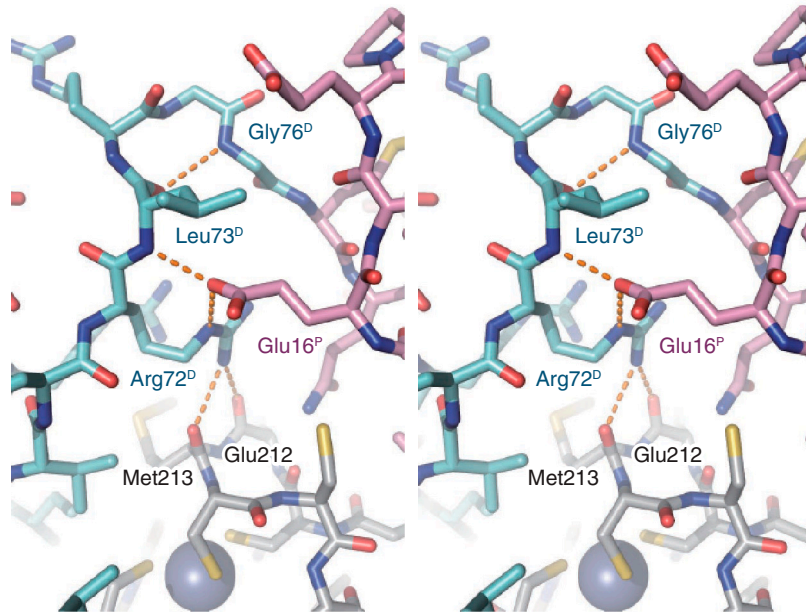


Fig. S8. Interactions between the distal and proximal ubiquitin moieties. Stereo view of the binding interface between the distal and proximal ubiquitin moieties. The coloring schemes are the same as in Fig. 2.

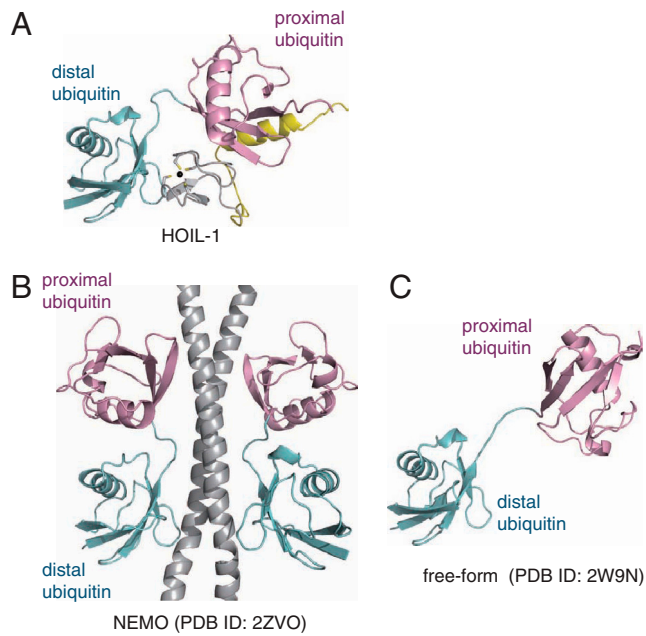


Fig. S9. Comparison of the crystal structures of the HOIL-1L-bound, NEMO-bound and free linear Ub₂ molecules. Coloring schemes are the same as in Fig. 2. (A) Crystal structure of the HOIL-1L•linear Ub₂ complex. (B) Crystal structure of the NEMO•linear Ub₂ complex. NEMO is colored gray. (C) Crystal structure of the free linear Ub₂.

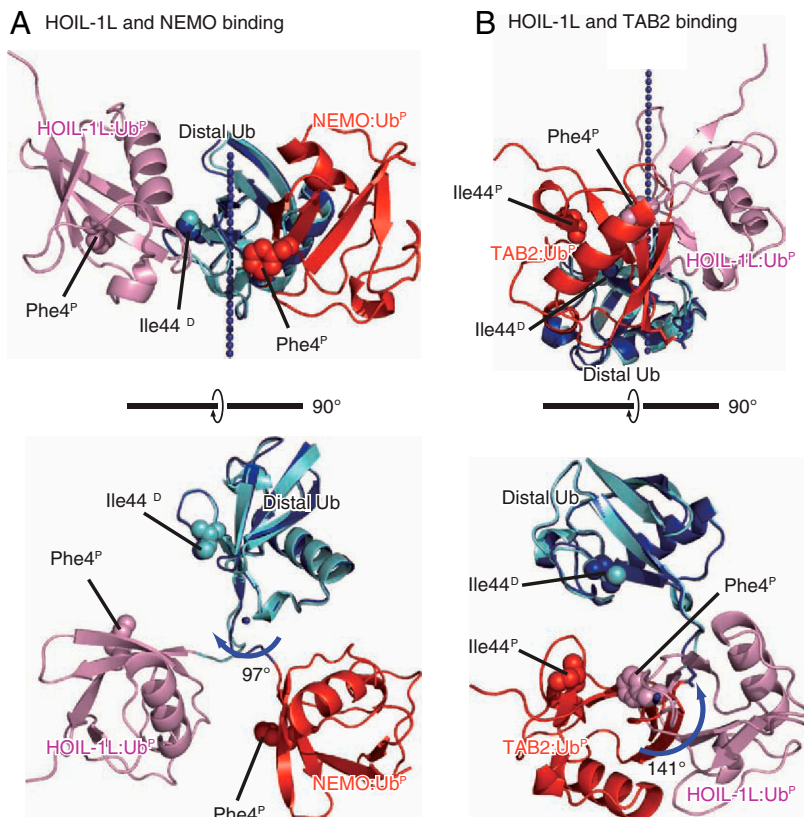


Fig. S10. Rotation of the proximal ubiquitin moieties. (A) Comparison between the HOIL-1L•linear Ub₂ and NEMO•linear Ub₂ complexes. The distal ubiquitin moiety in the NEMO•linear Ub₂ complex is superposed onto that in the HOIL-1L•linear Ub₂ complex. The distal and proximal ubiquitin moieties of the HOIL-1L•linear Ub₂ complex are colored cyan and pink, respectively, whereas those of the NEMO•linear Ub₂ complex are colored blue and red, respectively. The rotation axis of the proximal ubiquitin moieties is indicated as a dotted blue line. (B) Comparison between the HOIL-1L•linear Ub₂ and TAB2•K63-Ub₂ complexes. Drawing schemes are the same as in A, except that the NEMO•linear Ub₂ complex is replaced by the TAB2•K63-Ub₂ complex.

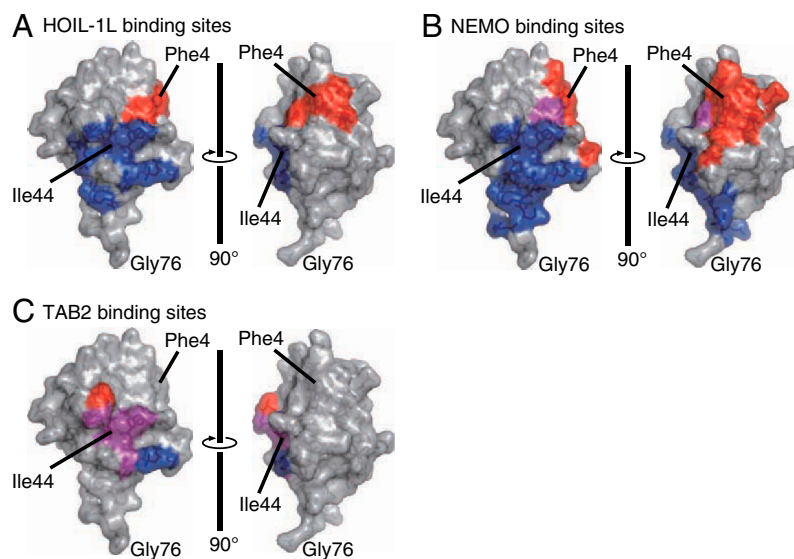


Fig. S11. Binding surfaces of diubiquitin. Binding surfaces on the distal and proximal ubiquitin moieties are highlighted by blue and red, respectively. Overlapped regions are highlighted by purple. (A) HOIL-1L-binding surfaces of linear Ub₂. (B) NEMO-binding surfaces of linear Ub₂. (C) TAB2-binding surfaces of K63-Ub₂.

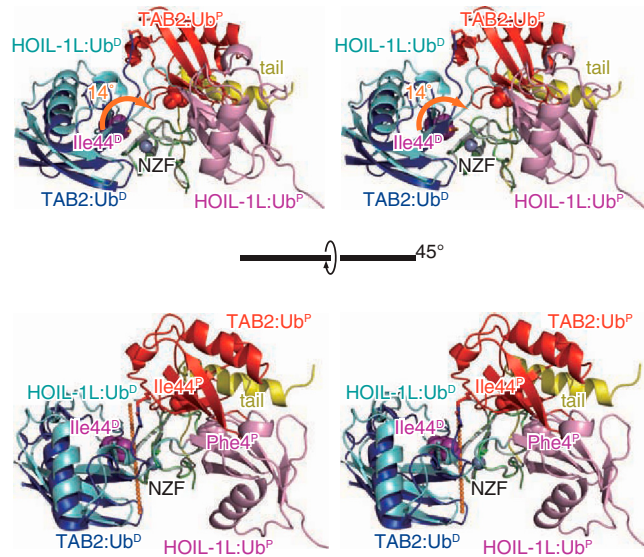


Fig. S12. Rotation of the distal ubiquitin moiety. The NZF core in the HOIL-1L•linear Ub₂ complex is superposed onto that in the TAB2•K63-Ub₂ complex. The NZF core and tail, and distal and proximal ubiquitin moieties in the HOIL-1L•linear Ub₂ complex are colored gray, yellow, cyan, and pink, respectively. The NZF, distal and proximal ubiquitin moieties in the TAB2•K63-Ub₂ complex are colored green, blue, and red, respectively. Ile44 residues of the distal ubiquitin moieties are shown as purple spheres. The rotation axis of the distal ubiquitin moiety is indicated as a dotted orange line.

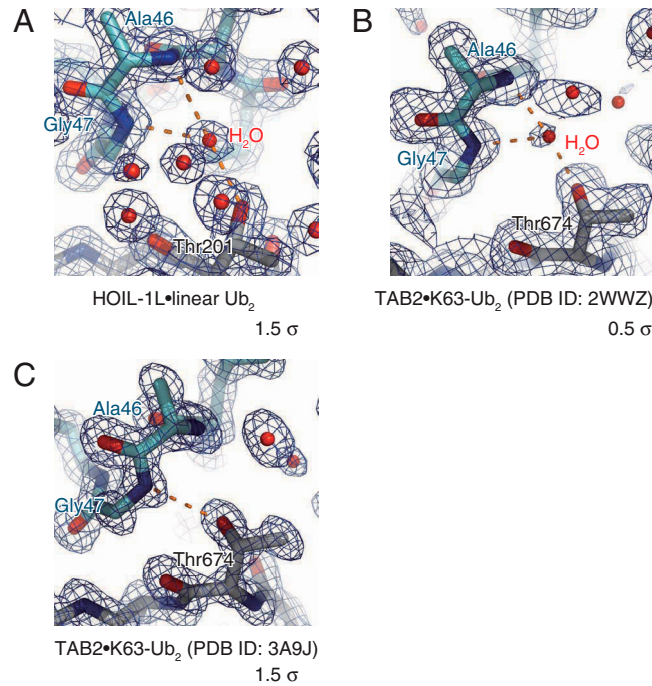


Fig. S13. Differences in the relative orientation between the distal ubiquitin and NZF domain. (A) The interface of the HOIL-1L NZF domain•linear Ub₂ complex; $2F_o - F_c$ electron density map contoured at 1.5σ (this work) is shown. The NZF domain and distal ubiquitin moiety are colored gray and cyan, respectively. Water molecules are shown as red spheres. Hydrogen bonds are indicated as dashed orange lines. Labels of the NZF domain and the distal ubiquitin moiety are colored black and cyan, respectively. (B) The interface of the Komander group's TAB2 NZF•K63-Ub₂ complex; $2F_o - F_c$ electron density map contoured at 0.5σ (8) is shown. Drawing schemes are the same as in A. (C) The interface of our TAB2 NZF•K63-Ub₂ complex. $2F_o - F_c$ electron density map contoured at 1.5σ (9) is shown. Drawing schemes are the same as in A.

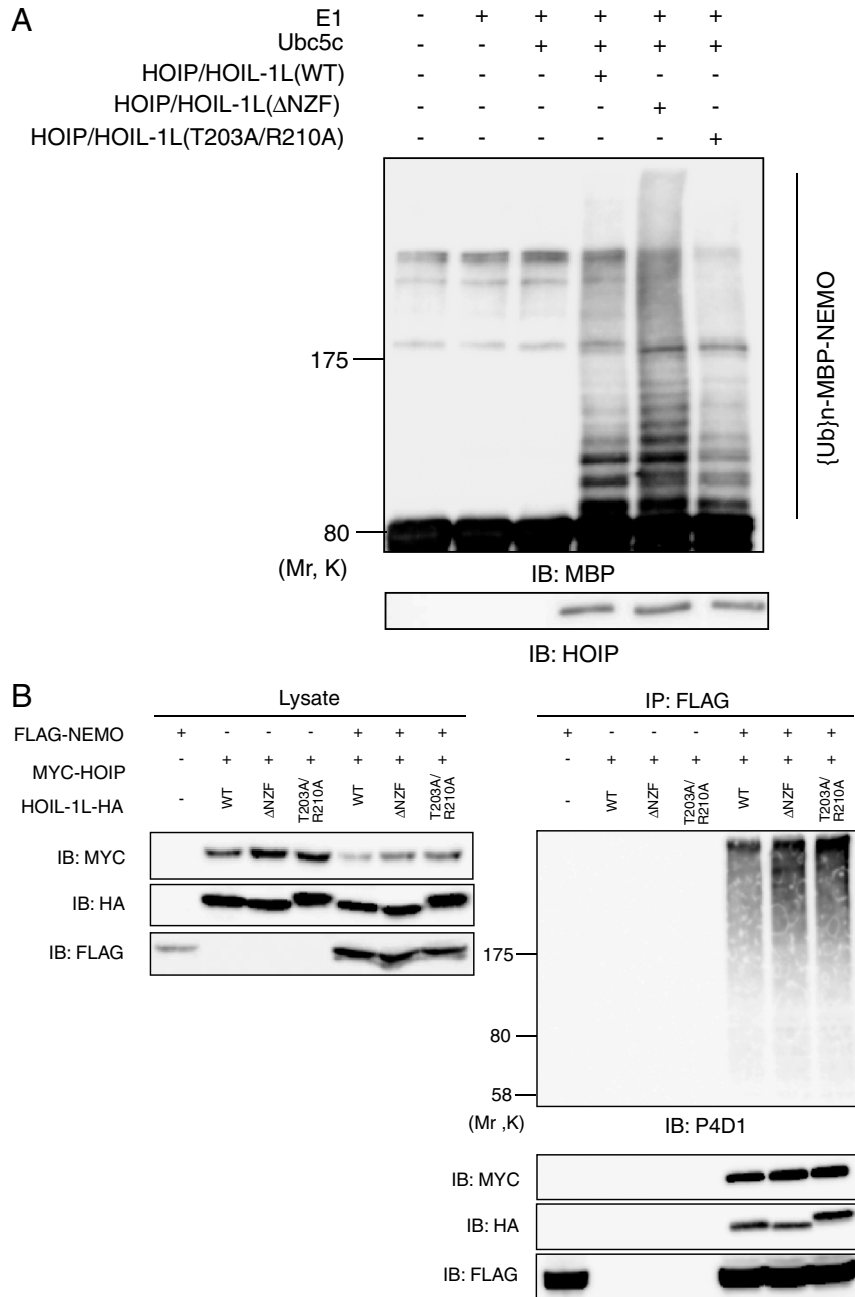


Fig. S14. Polyubiquitination of NEMO by LUBAC mutants. (A) Polyubiquitination of NEMO by LUBAC mutants in vitro. (B) Polyubiquitination of NEMO by LUBAC mutants in vivo.

Table S1. Data collection and refinement statistics

	Form I	Form II
Data collection		
Space group	<i>P4₃2₁2</i>	<i>P6</i>
Unit cell parameter	<i>a</i> = <i>b</i> = 104.9 Å, <i>c</i> = 170.4 Å	<i>a</i> = <i>b</i> = 113.7 Å, <i>c</i> = 75.7 Å
Wavelength, Å	1.28260	1.28260
Resolution, Å	50.0-1.70 (1.72-1.70)	50.0-1.90 (1.92-1.90)
Unique reflections	104,677	43,879
Total reflections	890,221	316,730
Completeness, %	97.5 (92.8)	98.8 (97.8)
<i>I</i> / σ (<i>I</i>)	43.88 (3.97)	37.3 (2.85)
<i>R</i> _{sym}	0.107 (0.319)	0.066 (0.309)
Refinement statistics		
Number of atoms: protein; compound; zinc; water	6,665; 46; 4; 830	3,355; 11; 2; 319
Rmsd bond length, Å	0.006	0.007
Rmsd bond angle, °	1.073	1.005
Average <i>B</i> factors (Å ²):protein, compound, zinc, water	23.6, 25.7, 22.4, 33.2	39.3, 40.7, 38.2, 41.5
Residues in core region, %	95.2	95.3
Residues in additionally allowed region, %	4.8	4.7
Residues in generously allowed region, %	0.0	0.0
Residues in disallowed region, %	0.0	0.0
<i>R</i> _{work} , <i>R</i> _{free}	0.174, 0.211	0.180, 0.227

The numbers in parentheses are for the highest resolution shell.

$$R_{\text{sym}} = \frac{\sum |I_{\text{avg}} - I_i|}{\sum I_i}$$

$$R_{\text{cullis}} = \frac{\sum ||FPH - FP| - |FH(\text{calc})||}{\sum |FPH|}$$

$$R_{\text{work}} = \frac{\sum |F_o - F_c|}{\sum F_o} \text{ for reflections of working set.}$$

$$R_{\text{free}} = \frac{\sum |F_o - F_c|}{\sum F_o} \text{ for reflections of test set (5\% of total unique reflections).}$$

Table S2. Details of the constructs used in this study

GST-pull down assay and SPR

UBDs	details of the constructs
HOIL-1L	mouse HOIL-1L (residues 192–250)
Δtail	mouse HOIL-1L (residues 192–220)
T201A	mouse HOIL-1L (residues 192–250, Thr201Ala)
R208A	mouse HOIL-1L (residues 192–250, Arg208Ala)
TAB2	mouse TAB2 (residues 665–693)
Npl4	mouse Npl4 (residues 549–576)
SHARPIN	mouse SHARPIN (residues 342–380)
NEMO	mouse NEMO (residues 249–343)
NF-kB assay	
Human HOIL-1L mutants	details of the constructs
WT	human HOIL-1L
ΔNZF core	ΔNZF core (residues 194–222) *equivalent to mouse HOIL-1L (Δ192–220)
Δtail	ΔNZF tail (residues 223–252) *equivalent to mouse HOIL-1L (Δ221–250)
SHARPIN	NZF core (residues 194–222) is swapped with mouse SHARPIN NZF (residues 342–370)
SHARPIN Δtail	NZF (residues 194–252) is swapped with mouse SHARPIN NZF (residues 342–370)
TAB2	NZF core (residues 194–222) is swapped with mouse TAB2 NZF (residues 665–693)
TAB2 Δtail	NZF (residues 194–252) is swapped with mouse TAB2 NZF (residues 665–693)
Npl4	NZF core (residues 194–221) is swapped with mouse Npl4 NZF (residues 549–576)
Npl4 Δtail	NZF (residues 194–252) is swapped with mouse Npl4 NZF (residues 549–576)
T203A	Thr203Ala *equivalent to mouse HOIL-1L Thr201Ala
R210A	Arg210Ala *equivalent to mouse HOIL-1L Arg208Ala
T203/R210A	Thr203Ala/Arg210Ala *equivalent to mouse HOIL-1L Thr201Ala/Arg208Ala
R239A	Arg239Ala *equivalent to mouse HOIL-1L Arg237Ala
E243A	Glu243Ala *equivalent to mouse HOIL-1L Glu241Ala
R239/E243A	Arg239Ala/Glu243Ala *equivalent to mouse HOIL-1L Arg237Ala/Glu241Ala